Design Approach for a Novel Multi Material Variable Flux Synchronous Reluctance Machine without Rare Earth Magnets

Julius Kesten[1], Felix Frölich[2], Florian Wittemann[2], Jonathan Knirsch[2], Florian Bechler[3], Luise Kärger[2], Peter Eberhard[3], Frank Henning[2] and Martin Doppelbauer[1]

Abstract—A method to design a variable flux electric machine using no rare earth materials is proposed. Starting from a synchronous reluctance machine's rotor the electromagnetic and mechanical design goals are derived. To improve torque production radially magnetized low coercive field magnets are inserted in the rotor, allowing for a control of the rotor flux. The flux guidance is improved by removing the webs required for mechanical sturdiness, which is achieved instead by mold injecting fiber reinforced polymer into the flux barriers. On the basis of a large design of experiments and using Gaussian process regression models, the relation between the rotor design parameters and output torque as well as external fields in the magnets is investigated and an optimization is performed. The resulting machine design allows an operation with high torque without involuntary demagnetization. The potential of the polymer filled flux barriers is confirmed through structural mechanical analysis.

Index Terms—Design of experiments, electric machines, finite element analysis, modeling, multi material design, optimization, reinforced polymers, rotor design, structural design

I. Introduction

Most of the traction motors in battery electric vehicles (BEV) rely on rare earth (RE) magnets, such as neodymium-iron-boron or samarium-cobalt, for torque generation. Due to the high remnant flux density B_{rem} and large coercive force H_{C} of the RE magnets they enable high torque and power densities and very good efficiencies. However, the mining of RE materials has drastic impacts on the local environment of the mines and production facilities, polluting water and contaminating the soil with radioactive radiation. [1].

Therefore, finding a replacement for the permanent-magnet synchronous machine (PMS) relying on these RE materials is a consequent step in reducing the ecological impact of BEV beyond CO_2 emissions alone. Alternative machine topologies include the induction machine (IM), the separately excited synchronous machine (SSM), the switched reluctance machine (SRM) and the synchronous reluctance machine (SynRM). The IM functions without any permanent magnet (PM) in the rotor, but it suffers from a low power factor and low power densities. The SSM generates torque with the help of a DC coil in the rotor creating a magnetic field. The need for charcoal brushes to connect the rotating coils leads to additional mechanical parts subject to wear. While there are approaches to design a SSM without charcoal brushes as presented in [2], the rotor winding still induces additional copper losses leading to reduced efficiencies compared to PSM. Relying solely on the principle of reduced magnetic energy, i.e. finding the path of minimal reluctance, the SRM works with simple and robust rotor structures without PM but requires an elaborate control while also suffering from large torque ripple.

The SynRM uses the same stator as a PSM or IM while also working with the reluctance principle. Its rotor is designed in a way that encourages the magnetic flux in one direction while prohibiting its expansion in the other direction. Like the SSM, the SynRM has no need for PM in the rotor. Therefore, both machine types have low power factors.

To improve the SynRM's power factor and torque production adding PM without rare earth materials has been proposed and closely investigated by many researchers. Considering the topology of the commonly used transversally laminated (TLA) SynRM, two approaches for improving torque production with PM can be defined based on the direction of magnetization in respect to the rotor: radially and tangentially magnetized magnets. In machine concepts with tangential magnetization the PM-field supports the flux and adds to the rotor's saliency, i.e. the ratio between the q-axis and the d-axis flux [3]. In radially magnetized systems the magnet flux adds to the d-axis flux and improves torque production in that way [4]. The difference between the two design concepts is displayed in Fig. 1.

PM materials commonly used in such machines are ferrite magnets or AlNiCo magnets. While the first have low remnant flux densities of around $B_{\mathrm{rem,Ferrite}} = 0.4\,\mathrm{T}$

and coercive forces of up to $H_{\mathrm{C,Ferrite}} = -400\,\mathrm{kA/m}$, the latter can compete with the rare earth SmCo magnets having flux densities of up to $B_{\mathrm{rem,AlNiCo}} = 1.1\,\mathrm{T}$, but only small coercive forces around $H_{\mathrm{C,AlNiCo}} = -120\,\mathrm{kA/m}$.
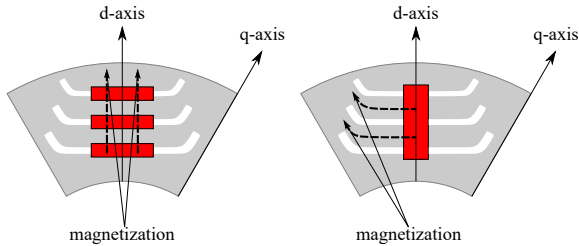
Fig. 1. Definition of the radial magnetization (left) and tangential magnetization (right).

However, the apparent disadvantage of the AlNiCo magnets can be used to an advantage. Owing to the low coercive force, it is possible to change the magnet's flux output, resulting in an additional degree of freedom (DOF) in controlling an electrical machine's torque. To do so, the field opposing the direction of magnetization must be increased sufficiently to push the BH-curve beyond the flexion point, resulting in the magnet returning to a working point of less flux density compared to the starting point. The opposing field is created and controlled via the stator current. This process is shown in Fig. 2.
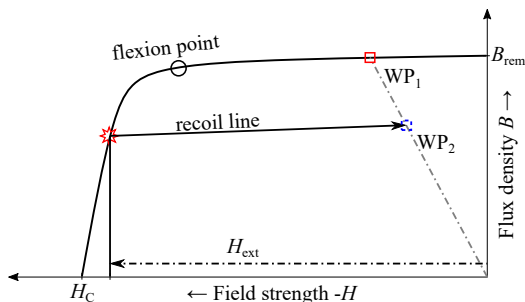
Fig. 2. Magnetization as a function of applied field.

The magnet in this qualitative representation is at working point WP_1 when no external field is applied. After application and release of the external field H_{ext} the magnet's working point is moved along the recoil line to the new working point WP_2 resulting in a reduced output flux density.

The same principle is applied to elevate the magnet's level of magnetization. In tha case, a positive external field of sufficient magnitude is applied, pushing the operating point along the recoil line to the outer loop in the first quadrant of the magnetization curve. If the field strenth is big enough, the new working point lies on a recoil line parallel to the previous one, resulting in a higher flux density.

By applying appropriate stator currents and thereby generating fields accordingly, it is possible to nearly instantaneously change the flux density of a machine's rotor. Investigation into this principle called "memory motor" or variable flux machine have been made and several approaches were proposed [5], [6]. In [7] a rotor is investigated with its PM flux consisting of the combination of rare earth magnets as wells as magnets with low coercive force allowing for a limited control of the machine's rotor flux. As a consequence of the high coercive force magnets it is not possible with this machine design to benefit fully from the possible improvement in efficiency under partial load in the field weakening region. While the rotor geometry in the previously discussed paper is similar to the salient pole configuration of an SSM with the high coercive and low coercive force magnets stacked on top of each other at the pole caps, the rotor geometry proposed in [8] has one radially magnetized high coercive force magnet per pole in the d-axis close to the shaft and one tangentially magnetized low coercive force magnet in the q-axis as defined in Fig. 1. In [6] a variable flux machine is designed relying solely on AlNiCo magnets. Here, the use of AlNiCo9 which has comparably high coercive force of $H_{\mathrm{C}} = -112\,\mathrm{kA/m}$ and remnant flux density $B_{\mathrm{rem}} = 1.05\,\mathrm{T}$ is proposed. The flexion point lies at around $-90\,\mathrm{kA/m}$. The magnetization of the rotor is tangential, leading to a drastic loss of torque once the the PM-flux is reduced, because there is only little reluctance torque.

Considering the drawbacks and advantages of the machines described the aim of the topology proposed in this work is to benefit from as many advantageous properties as possible while eliminating the drawbacks. Therefore, a novel methodology using statistical modeling and mathematical optimization for the design of an innovative multi material machine concept is presented in within this work. The machine concept employs the rotor of a synchronous reluctance machine adding AlNiCo magnets to it, in that way creating a variable flux synchronous reluctance machine (VF-SynRM). To improve speed strength, the rotor's flux barriers are injected with fiber reinforced polymer.

II. Design Approach

To achieve high torque production without any PM flux a SynRM rotor is selected as the starting point. According to [9] the SynRM efficiency η can be approximated using

$$\eta \approx \left(1 + \frac{P_{\mathrm{Cu}}}{\omega_{\mathrm{r}} T}\right)^{-1} \qquad (1)$$

with copper losses P_{Cu}, rotor rotational speed ω_{r} and electromagnetic torque T. Replacing $P_{\mathrm{Cu}} = 3R_S I_S^2$ with the stator resistance R_{S} and the stator current I_{S} Eq. 1 can be reformulated to:

$$\eta \approx \left(1 + \frac{1}{\frac{\omega_{\mathrm{r}}}{3 \cdot R_{\mathrm{S}}} \cdot \frac{T}{I_{\mathrm{S}}^2}}\right)^{-1}. \qquad (2)$$

While not considering any iron or mechanical losses Eq. 2 reveals an important relation: A SynRM's efficiency is

elevated by either increasing the torque generated per stator current (T/I_S^2) or by increasing the motor speed ω_r. This work focuses on both aspects while regarding the respective mechanical and electromagnetic restrictions. The rotor design of VF-SynRM, just like any SynRM, needs to respect the opposing goals of mechanical strength allowing for high speeds and good magnetic conductivity along the q-axis as defined in Fig. 1 with the electromagnetic torque of a PM-assisted SynRM given as

$$T = \frac{3}{2}p \cdot (\Psi_{PM} \cdot i_q + (L_d - L_q) \cdot i_d i_q) \tag{3}$$

with the number of pole pairs p, the permanent magnet flux Ψ_{PM}, the inductances in the d- and q-axes L_d and L_q and the current components i_d and i_q. As discussed in numerous publications, a high torque is achieved by maximising the saliency, i.e. the ratio L_q/L_d. Many proposals on optimizing the classical SynRM's rotor with respect to improved saliency have been made. The webs granting stability between the iron paths are counterproductive in achieving this goal, as they provide paths for undesirable d-flux Ψ_d. To eliminate this counterproductive effect, the machine considered in this paper will be designed without the webs leading to a decrease of mechanical strength. In order to achieve the design goal of high speed despite the missing webs the flux barriers of the machine will be injected with fiber reinforced polymer granting additional sturdiness. The second design goal is increasing the torque per current T/I_S^2. This goal is partially achieved by removing the rotor webs. To increase torque output further AlNiCo9 magnets are embedded in the flux barriers. By doing so not only is there an increase in torque due to the magnets' flux, but the opportunity to control the magnet flux opens up as well. As described in Section I the magnets' low coercive force permits only small magnitudes of current (and thereby magnetic field strength) since large magnitudes result in an unwanted change of magnetization. It is therefore critical to design the machine's rotor in a way that allows a current as high as possible without pushing the magnets past the flexion point, thus increasing the torque per current relation as much as possible.

A. Electromagnetic method

Two main electromagnetic design goals for the machine's rotor design can be derived: Maximum mechanical sturdiness without the iron webs and as much torque T as possible utilizing as much stator current I_S as possible without demagnetizing the magnets. These goals pose a multi-objective optimization problem. Since the optimization goals are of mechanical as well as electromagnetic nature the design process is divided into three sections. First, the design space for the electromagnetic optimization is restricted by identifying mechanical boundary conditions. With the constraints defined, a variety of machine geometries is specified using latin hypercube sampling (LHS) as means of design of experiments (DOE). The electromagnetic characteristics of all machines are calculated using a finite element analysis

(FEA) toolchain the results of which are then used as the data to be optimized using a genetic algorithm (GA). In the final step the optimized machines are evaluated according to their mechanical suitability and the best one is selected.

The focus of this work lies on the second step, i.e. the electromagnetic DOE and the optimization strategy. To reduce the DOF in the optimization the machine's stator is not varied. A parameterized rotor model is used for the LHS design. The model consists of 13 parameters. The template for this optimization was taken from the commercial Software FluxMotor 2019.1 by Altair. A selection of the parameters and the general rotor topology are presented in Fig. 3. Parameters referring to different magnets but describing the same quantity (e.g. WMA, WMB and WMC) are displayed only once for the sake of clarity in the picture.
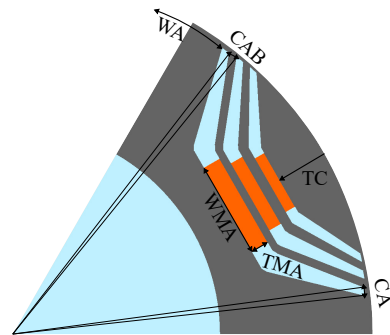
Fig. 3. Rotor geometry and parameters used for the design process.

When creating a DOE based on any statistical sampling method the proper choice of sample size is crucial. The relation between sample size and variables examined defines the amount of computational time required and the statistical significance of the resulting model. According to [10] the relation between total sample size $N = \alpha \cdot M$ with α being the number of respective samples and M being the size of each sample and number of variables k should be at least $M/k > 10$, with $\alpha > 5$. The statistical significance of the sample may also be improved by enlarging N while $\alpha = 1$, as it also reduces computational effort. In the present case the sample size is chosen as $N = 1000$ with $k = 13$ being the rotor parameters.

With the simulations completed, the relation between the varied parameters and the outputs of interest needs to be modeled to achieve a motor geometry that fulfils the design goals mentioned above by optimizing the parameters k. The main optimization goal in the electromagnetic domain is the maximum possible generation of torque T for a given current I_S. Maintaining a stable magnet working point is the secondary goal.

Both quantities are modeled using Gaussian process regression (GPR) models, which allow precise predictions of noisy data, being non-parametric. This regression technique enables mapping a set of input data $\boldsymbol{x}$ to an output variable y using probabilistic methods. In case of the present machine design $\boldsymbol{x}$ is given through the $N = 1000$ variations of each of the

$k = 13$ rotor parameters, resulting in a 13×1000 matrix, whereas y is the quantity to be modeled. The resulting model is then able to predict an output parameter $\hat{y}$ with a given input set $\boldsymbol{x}$ [11].

$N_{\mathrm{train}} = 800$ datasets are employed to train the GPR model, while the remaining $N_{\mathrm{test}} = 200$ are test data. The training and test data are randomly selected from the $N = 1000$ machines. To test model quality, the mean squared error (MSE) of the test data's prediction is used, comparing the model's output $\hat{y}$ from the input test data $\boldsymbol{x}_{\mathrm{test}}$ to the actual output y_{test}.

The torque T is modeled using a normalized representation

$$T_{\mathrm{norm}} = \frac{T_{\mathrm{i}}}{T_{\mathrm{mean}}} \tag{4}$$

with T_{mean} being the mean value of torque T over all $N = 1000$ datasets. With $MSE_{\mathrm{T}} = 4.0652 \times 10^{-6}$ the model quality is good. Figure 4 shows the actual torque values T_{test}, the modeled values $\hat{T}$ and the 95% prediction interval of the respective observation for 25 machine designs from the test dataset.
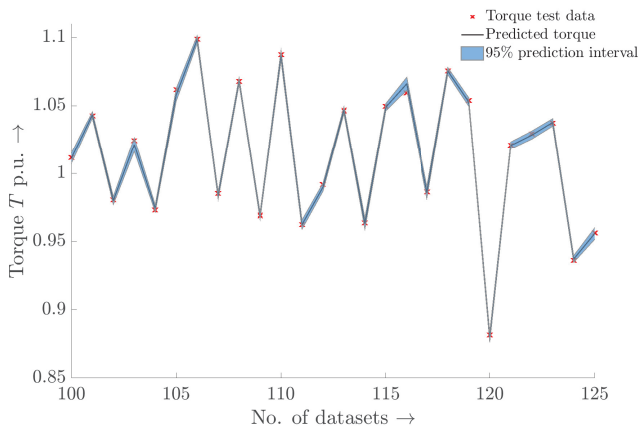
Fig. 4. GPR fit of machine torque vs. actual torque with prediction interval.

The 95% prediction interval represents the area in which the true response value of an observation $\boldsymbol{x}$ will lie with a certainty of 95%.

The external fields in the magnets are selected as nonlinear constraints in the optimization. Since the simulation of the machine characteristics is discretised into 5 points in the current I_{S} and 6 points in the current angle φ domain, the area and time averaged external fields for each magnet are represented by 5×6 matrices. To effectively apply the constraints, this discretisation is put to use by restricting the number of field values in each 5×6 matrix which have a magnitude larger than that of the flexion point to be $n_{PM,i} < 1$ for either of magnets. To reduce the amount of points being modeled for each magnet only those $I_{\mathrm{S}} - \varphi$ pairs that are required for base speed operation are used for modeling, as the magnet flux Ψ_{PM} is reduced in most of the field weakening range, resulting in a shift of the flexion point

to the left, compare Fig. 2. The model quality of the models applied for the magnetization is still acceptable although the maximum error of the three models $MSE_{\mathrm{PM1}} = 0.5675$ for the innermost magnet is considerably higher than that of the torque model.

All models presented in this section were created using an automatic hyperparameter optimization with the squared-exponential kernel function for the acquisition of the covariance matrix. The modeling and optimization were carried out using Matlab® R2020a. The GA is then applied to the torque model as optimization goal and the magnet models as nonlinear constraints. The algorithm evaluates the target function consisting of the GRP model of the torque T with several randomly selected set of input data $\boldsymbol{x}$ within the predefined borders, i.e. the upper and lower limits for each of the $k = 13$ rotor parameters. The resulting estimated torque values $\hat{T}$ are then compared to each other and the estimation of magnet workings points beyond the flexion point $\hat{n}_{\mathrm{PM,i}}$ for each magnet. From this population, those individuals with the best performance considering the optimization goal and the constraints are selected and a new set of data is created, mixing individuals from the preceding generation and adding new ones, resulting in a new population to be evaluated. This process is repeated either until an individual, i.e. a machine design, satisfying the requirements is found or until a predefined stop criterium is met [12]. The optimizer suggests several sets of rotor parameters which are then simulated using FEA.

Because this work presents the steps undertaken in designing the VF-SynRM, the electromagnetic data is normalized to the base speed and base speed torque of the optimized, simulated machine.

B. Mechanical method

To investigate the potential of polymer-filled flux barriers, a 2D simulation of a section of the electromagnetic optimized rotor is performed with both polymer-filled and non-filled flux barriers. The simulation is made using the software package Abaqus 2021 HF7 from Dassault Systèmes Simulia. The cyclically symmetrical section of the rotor is simulated as a plane strain problem. The section angle is $60\,^{\circ}$. Linear quadrilateral elements of type CPE4R are selected.

In these simulation, it is assumed that all materials are isotropic linear elastic. The polymer used is a glass fiber reinforced polyphenylene sulfide (PPS) with 20% fiber volume content. Characteristic values similar to steel are selected for the electrical steel sheet. Standard literature data are used for the characteristic data of the two mentioned materials as well as of the magnets. Tab. I summarizes the material properties required for the calculation. To map the cyclic symmetry, the respective edges of the subsection are linked with a cyclic symmetry boundary condition. With respect to a specified symmetry axis in the coordinate origin of the geometry in the direction of the z-axis, corresponding displacements are coupled or locked tangentially as well as radially of the rotor. The number of symmetrical sections per

full circle is specified as the sector number (total number of sections) depending on the section angle. In this case, the number corresponds to six.

To ensure static determination, the displacement of the two corner points located at the inner radius in tangential direction is suppressed. Since the real rotor is only axially pressed and not glued to the shaft, it is not assumed that the rotor transmits forces in radial or tangential direction via the inner radius.

By injecting the polymer directly onto the heated electrical sheet and then cooling it, adhesive, force-transmitting interface pairs are to be formed. All connected surfaces are therefore provided with a contact property that allows neither tangential sliding nor normal separation or penetration of the contact surfaces.

To simulate the loads on the rotor at maximum speed, a rotational body force with centrifugal load effect is used. The assumed maximum speed in revolutions per minute $n_{max} = 15\,000\,1/\text{min}$ corresponds to about $1570.8\,\text{rad/s}$. The axis of rotation is defined as equal to the axis of symmetry from the coordinate origin of the geometry in the direction of the z-axis. The linear approach is chosen as the loading curve over the time step. This allows the reliable convergence of the simulation. This load corresponds to the radius- and density-dependent volume force on the rotor due to inertia at a constant speed. It does not represent the inertial effect of acceleration for the rotor. Also, no load in the circumferential direction is introduced in this model to represent the magnetic force in operation. In addition to the resulting v. Mises stresses in the electrical sheet, this 2D model is also used to calculate the stresses on the resulting interface. Since experimental investigations of this interface are not part of this work, no evaluation of the load on the interface is made here, but only a potential for an increase in speed-strength is described under the background of a possible low interface load.

TABLE I
MATERIAL PROPERTIES FOR THE STRUCTURAL SIMULATION.

Material	Young's modulus	Poisson Ratio	Density
PPS GF20	6 GPa	0.34	$1.48\,\text{g/cm}^3$
electrical sheet	210 GPa	0.3	$7.56\,\text{g/cm}^3$
magnet	180 GPa	0.3	$7.25\,\text{g/cm}^3$

III. RESULTS

A. Electromagnetic results

The resulting geometry should achieve a high torque compared to the mean value of the DOE and have working points for the magnets below the flexion point, namely $H_{ext} \geq -90\,\text{kA/m}$. The optimization's effect on the torque T is presented in Fig. 5, where the normalized torque for all machine designs in the DOE is compared to the actual torque output of the optimized motor. In addition to the median value the 25th and 75th percentile are presented. While the optimized machine does not present the highest output torque, it lies on the 88.4th percentile, meaning it has

a higher torque output than $88.4\,\%$ of machines in the dataset. A comparison of the external fields in the magnets for the
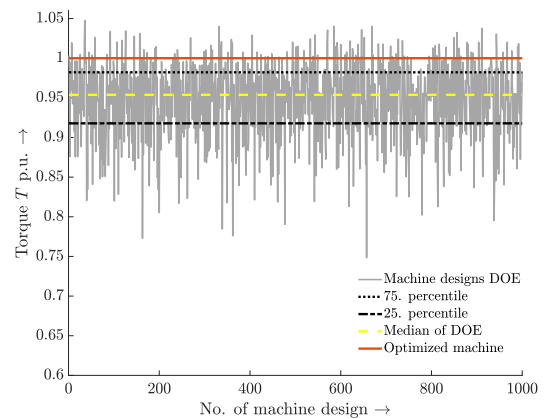
Fig. 5. Relative torque of the optimized machine compared to all machines in the DOE.

optimized machine to the design with highest output torque ($4.7\,\%$ more torque) reveals the impact of the constraint on the optimization, which was conducted for a fixed stator current I_S. The comparison can be seen in Fig. 6, where the maximum magnitude for the demagnetizing fields is presented. Here, the effect of the optimization is well visible. The external fields in the design with the highest torque exceed the permissible value by more than $26\,\%$ in PM1 and PM3.
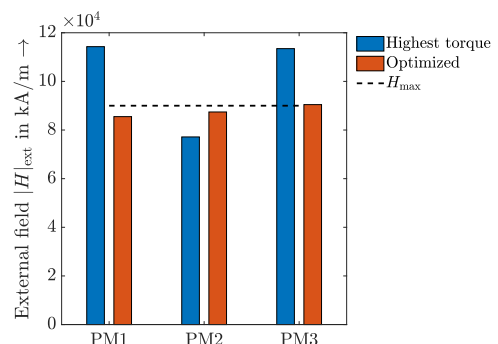
Fig. 6. External fields for the machine with highest torque and the optimized machine.

For the optimized machine, the external fields are within the boundary set by the magnetization curve of AlNiCo9 magnets. Since the machine design approach proposed here should be applicable for VF-SynRMs, Fig. 8 shows the comparison between the machine operating at full PM flux (PM mode), i.e. nominal flux of the AlNiCo magnets - machine operates as a PMS, and with no rotor flux (reluctance mode), i.e. zero flux produced by the AlNiCo magnets - machine operates as a SynRM. Note, that the torque envelopes presented in Fig. 8 display only static levels of magnetization, thereby comparing the machine efficiency for both operating modes. However, dynamic processes of change in magnetization

state are not presented. While the maximum torque during reluctance operation is by $22\,\%$ lower than in PM mode, the constant power speed range (CPSR) is very small when operating the machine as a reluctance motor. With the PM flux adding to the torque the machine's power is nearly constant over the complete speed range.

However, the results presented in Fig. 8 compare the machine designs only for operation with a magnitude of I_S causing no shift in the level of magnetization. To achieve higher torques, it is possible to raise the current and drive the machine with reduced Ψ_{PM} up to zero flux. The effects of supporting the torque generation using magnet flux on the machine efficiency lead to a slight improvement from $\eta_{rel} = 95.65\,\%$ to $\eta_{PM} = 97.0\,\%$. Also, the area of $\eta > 95\,\%$ is clearly enlarged in PM mode.

B. Structural simulation results

Two failure critical areas are identified: In the area where the bottom two corners of the innermost magnet touch the electrical sheet and at the thinnest part of the sheet at the outermost edge of the rotor. Both areas are shown enlarged in Fig. 7 for both, a rotor with polymer-filled flux barriers and an unfilled rotor.
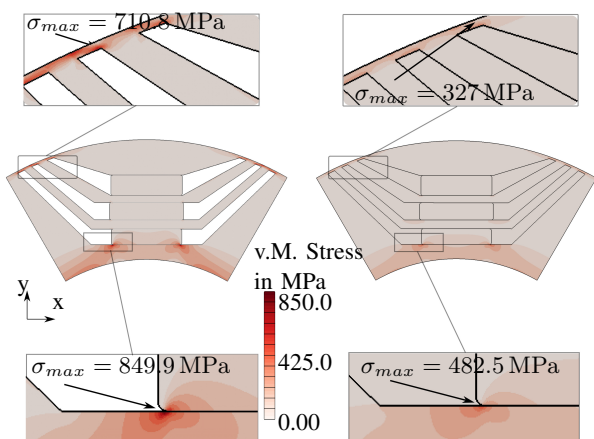
Fig. 7. Failure critical regions are shown enlarged, both for an unfilled rotor (left) and a rotor with polymer-filled flux barriers (right).

The simplified structural simulation showed that injecting the flux barriers with a fiber reinforced thermoplastic can significantly increase the speed-strength of the rotor. In the outer failure-critical area of the electrical sheet, the maximum stress could be reduced by approx. $54\,\%$.

In the inner failure-critical area, the stress can be reduced by approx. $43.23\,\%$. However, it should be noted that locally strongly increased stresses could be attributed to numerical singularities. In any case, the geometry of the rotor must be adapted locally in this area to avoid increased stresses.

The tensile load at the interface between the polymer and the electrical sheet is always below $30\,\mathrm{MPa}$ and the shear load below $25\,\mathrm{MPa}$. Whether such an interfacial strength can be achieved with the described injection molding of the polymer must be investigated in further experimental studies.

A stiffer polymer would further increase the speed-strength. However, it leads to higher stresses at the interfaces. Based on the experimental results, the rotor can be fully mechanically designed and a maximum possible increase in speed-strength can be determined.

IV. Conclusion

The goal of this work was to present a design method for a variable flux synchronous reluctance machine (VF-SynRM) taking into account electromagnetic optimization goals and mechanical design restrictions. The first scope is achieved by creating a DOE and modeling the rotor parameters' relation to the torque and the external fields in the AlNiCo magnets and using these results as the basis for an optimization. A genetic algorithm is used to conduct the optimization. The modeling of torque and external fields is done using GPR models with reasonable results. The final machine design achieves high torque in comparison to all machines in the DOE while also keeping the magnets' working points stable. As a conventional SynRM was the starting point for this investigation, the performance of the final machine design with full PM flux and no PM flux is presented, revealing a $22\,\%$ increase in torque and an efficiency elevated by $1.35\,\%$. With these general steps in place and the validation of functionality, the presented optimization approach can be extended to a multiobjective algorithm incorporating additional design goals like a cycle efficiency or the torque ripple.

The mechanical approach focuses on enhancing the speed strength of the machine by filling the flux barriers with fiber reinforced polymer. This grants a reduction of maximum mechanical stress by $54\,\%$ in the outer failure-critical area of the rotor. In the inner failure-critical area, a reduction by $43.23\,\%$ is achieved. However, the local stress peaks require local adjustments to the rotor geometry. Also, interfacial strengths must be determined experimentally. A prediction of the final speed strength of the rotor can be given based on these results. Furthermore, injection molding simulations need to be carried out to ensure a proper injection process. In [13] a promising approach for the simulation of injection molding processes with fiber reinforced polymers is presented.

Owing to the variable rotor flux of the machine design, the NVH behaviour requires special attention. The method to model the NVH behavior of electric machines presented in [14] allows fast and accurate prediction of critical sonic paths.

References

[1] A. Walters and P. Lusty, "Rare earth elements profile," *British Geological Survey*, 2010.

[2] Q. Long, Z. Zhou, X. Lin, and J. Liao, "Investigation of a novel brushless electrically excited synchronous machine with arc-shaped rotor structure," *Energy Reports*, vol. 6, pp. 608–617, 2020.

[3] S. S. Maroufian and P. Pillay, "Pm assisted synchronous reluctance machine design using alnico magnets," in *2017 IEEE International Electric Machines and Drives Conference (IEMDC)*. IEEE, 21.05.2017 - 24.05.2017, pp. 1–6.
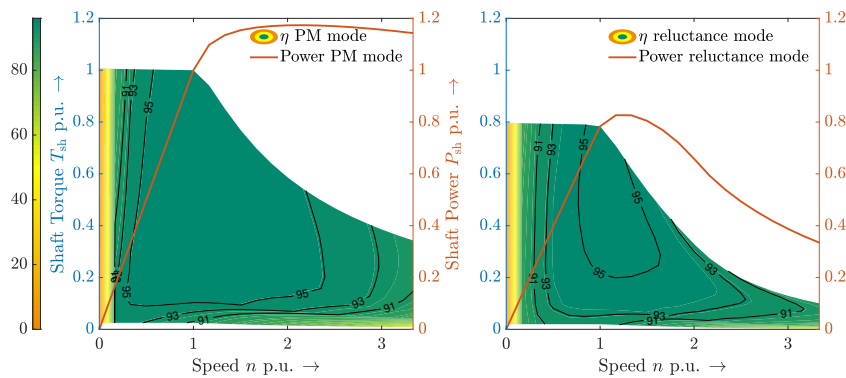
Fig. 8. Machine characteristics for PM mode and reluctance mode.

[4] T. A. Huynh, M.-F. Hsieh, K.-J. Shih, and H.-F. Kuo, "An investigation into the effect of pm arrangements on pma-synrm performance," *IEEE Transactions on Industry Applications*, vol. 54, no. 6, pp. 5856–5868, 2018.

[5] V. Ostovic, "Memory motors," *IEEE Industry Applications Magazine*, vol. 9, no. 1, pp. 52–61, 2003.

[6] M. Ibrahim, L. Masisi, and P. Pillay, "Design of variable-flux permanent-magnet machines using alnico magnets," *IEEE Transactions on Industry Applications*, vol. 51, no. 6, pp. 4482–4491, 2015.

[7] A. Athavale, K. Sasaki, B. S. Gagas, T. Kato, and R. D. Lorenz, "Variable flux permanent magnet synchronous machine (vf-pmsm) design methodologies to meet electric vehicle traction requirements with reduced losses," *IEEE Transactions on Industry Applications*, vol. 53, no. 5, pp. 4318–4326, 2017.

[8] K. Sakai, K. Yuki, Y. Hashiba, N. Takahashi, and K. Yasui, "Principle of the variable-magnetic-force memory motor," in *2009 International Conference on Electrical Machines and Systems*. IEEE, 112009, pp. 1–6.

[9] M. J. Kamper, F. S. van der Merwe, and S. Williamson, "Direct finite element design optimisation of the cageless reluctance synchronous machine," *IEEE Transactions on Energy Conversion*, vol. 11, no. 3, pp. 547–555, 1996.

[10] A. Matala, "Sample size requirement for monte carlo - simulations using latin hypercube sampling," Thesis, Helsiniki University of Technology, Helsinki, 2008.

[11] K. P. Murphy, *Machine learning: A probabilistic perspective*, ser. Adaptive computation and machine learning series. Cambridge, Massachusetts and London, England: The MIT Press, 2012.

[12] Y. J. Cao and Q. H. Wu, "Teaching genetic algorithm using matlab," *The International Journal of Electrical Engineering & Education*, vol. 36, no. 2, pp. 139–153, 1999.

[13] F. Wittemann, L. Kärger, and F. Henning, "Theoretical approximation of hydrodynamic and fiber-fiber interaction forces for macroscopic simulations of polymer flow process with fiber orientation tensors," *Composites Part C: Open Access*, vol. 5, p. 100152, 2021.

[14] F. Bechler, J. Kesten, F. Wittemann, F. Henning, M. Doppelbauer, and P. Eberhard, "Simplified modeling of electromagnets for dynamic simulation of transient effects for a synchronous electric motor," *International Journal of Mechanical System Dynamics*, vol. 1, no. 1, pp. 89–95, 2021.

V. Biographies

Julius Kesten received his M.Sc in Mechatronics and Information Technology 2020 from the Karlsruhe Institute of Technology (KIT), Germany. Since 2020 he works at the Institute of Electrical Engineering at the KIT. His research interests include the design of synchronous reluctance and variable flux machines and the numerical optimization of electric machines.

Felix Frölich received his M.Sc. degree in mechanical engineering in 2021 from KIT and is now a Ph.D. student in the Institute of Vehicle System Technology at the KIT, starting 2021. His research interests are developing simulation models of additive manufacturing processes. In particular, he is working on the modeling of Fused Filament Fabrication on multi-size scales.

Florian Wittemann received M.Sc. in mechanical engineering in 2016. In 2021 he received his Ph.D. at the Institute of Vehicle System Technology chair of Lightweight Technology of the KIT. His research focus is the flow modeling of discontinuous fiber reinforced polymers with main focus on the fiber matrix interactions during mold filling.

Jonathan Knirsch received his B.Sc. in mechanical engineering in 2021. He is currently working towards his M.Sc.. His research interests include the multi-material desgin of electric machines and the analysis of contact surfaces.

Florian Bechler received his M.Sc. degrees in Engineering Cybernetics from the University of Stuttgart, Germany, in 2020. He is currently a doctoral student and a member of the research staff at the Institute of Engineering and Computational Mechanics at the University of Stuttgart. His research interests include modeling of multibody systems dynamics, and multi-disciplinary systems.

Luise Kärger is a Tenured Senior Scientist and Deputy Head of the Lightweight Technology Department at the Institute of Vehicle System Technology at KIT. Her research focus is on modelling and simulation of manufacturing processes of polymer and fiber reinforced composite components.

Peter Eberhard is full professor and since 2002 director of the Institute of Engineering and Computational Mechanics (ITM) at the University of Stuttgart, Germany. He was Treasurer and Bureau member of the International Union of Theoretical and Applied Mechanics, and served before in many national and international organizations, e.g., as Chairman of the IMSD (International Association for Multibody System Dynamics) or DEKOMECH (German Committee for Mechanics).

Frank Henning is professor and director at the Institute of Vehicle System Technology chair of Lightweight Technology of the KIT since 2008 and associate research professor at the Institute of Mechanical and Materials Engineering of the Western University, Canada since 2010. He is deputy director of the Fraunhofer institute of chemical technology Pfinztal, Germany and since 2016 he is president of the SAMPE Germany e.V.. He leads the Fraunhofer project centers in Ulsan, Korea and London, Ontario, Canada.

Martin Doppelbauer is full professor since 2011 at the Institute of Electrical Engineering (ETI) at the KIT. He holds a chair for Hybrid Electric Vehicles. Most recently he worked as head of electrical machine development at SEW Eurodrive GmbH in Bruchsal. Martin Doppelbauer is also active in national and international standardization and the chairman of IEC Technical Committee 2 Rotating Electrical Machines.